CHINESE OPTICS LETTERS

Vol. 21, No. 11 | November 2023

Femtosecond laser writing of low-loss three-dimensional waveguide coupler in $LiNbO_3$ crystal

Jinman Lü (吕金蔓)[1*], Ge Li (李 戈)[1], Yujie Ma (马钰洁)[1], and Feng Chen (陈 峰)[2]

[1] Shenzhen Key Laboratory of Ultraintense Laser and Advanced Material Technology, Center for Advanced Material Diagnostic Technology, and College of Engineering Physics, Shenzhen Technology University, Shenzhen 518118, China

[2] School of Physics, State Key Laboratory of Crystal Materials, Shandong University, Jinan 250100, China

*Corresponding author: lvjinman@sztu.edu.cn

Received April 19, 2023 | Accepted June 26, 2023 | Posted Online November 1, 2023

With different interactions between material and femtosecond lasers, two-dimensional (2D) and three-dimensional (3D) waveguide couplers, whose separation distances are fabricated in *z*-cut lithium niobate crystal by femtosecond laser writing, are reported. Experimentally and numerically, it is shown from results that the guidance is only propagating along TM polarization due to the Type I modification and holds equal splitting ratios, which are the same as power splitters at 632.8 nm. The propagation losses of 2D and 3D waveguide couplers exhibit better transmission properties than those of the previously reported Type I Y-junction waveguide splitters.

Keywords: femtosecond laser writing; beam splitters; lithium niobate.
DOI: 10.3788/COL202321.112201

1. Introduction

Miniaturized waveguide devices based on dielectric crystals have a significant role as the basic components in integrated photonics, owing to their small volumes for relatively high optical intensities confinement and combination of versatile bulk features[1–4]. As the best known and most widely researched optical waveguide device, an optical coupler can implement a number of applications in optoelectronics and integrated optics, such as power divider, optical switch, modulator, and filter[5–7]. Based on the existence of evanescent mode fields between two close-spaced waveguide lines, the light beam energy coupled into directional couplers can readily pass through one waveguide into another waveguide. Hence, the directional coupler can transmit light waves with reduced propagation loss.

The lithium niobate ($LiNbO_3$) crystal is the most widely applied electro-optic and nonlinear crystal for many multifunctional platforms. These include use as switches, electro-optic modulators, multiplexers, frequency converters, and waveguide amplifiers, benefiting from the crystal's unique electro-optic, piezoelectric, acousto-optic, and nonlinear optical properties[8–12]. Traditional methods exist for the manufacture of a perpetual waveguide coupler in this material, e.g., titanium or zinc indiffusion[13,14], dielectric periodic multilayers[15], proton exchange[16], and ion implantation combined with femtosecond laser ablation[17]. However, three-dimensional (3D) waveguide couplers are difficult to be fabricated by these techniques as they are all limited to the surface processing of samples. Since 1996, femtosecond laser writing (FLW) has been utilized in a variety of applications and shown its distinct and efficient capabilities for 3D processing in many transparent materials[18–21]. Due to the femtosecond laser's diverse irradiation parameters and transparent materials of differing lattice properties, the configuration of the waveguide can be briefly classified into two types of modifications according to the positive ($+\Delta n$) or negative ($-\Delta n$) refractive index changes in laser-irradiated tracks, i.e., Type I and Type II modifications, respectively[22,23]. For Type I modifications, the waveguide was located inside the region of directly written laser tracks, while the Type II waveguide was located in the adjacent regions of laser-written tracks. Recently, evanescent couplers with Type II modifications in $LiNbO_3$ crystal have been fabricated by FLW[24]. Nevertheless, Type II strong-damaged tracks restrained evanescent fields, leading to increased losses of 4 dB/cm, as described in Ref. [24]. Therefore, the mode coupling could only be realized between sufficiently weak structures or two close-spaced Type I waveguides. Type I waveguide couplers having no damage track to block next-neighbor coupling have been attributed to evanescent mode fields outside the couplers. Moreover, Type I modification has been found to be much easier than Type II configuration for the 3D fabrication of complex waveguide devices. In fact, waveguide coupling by FLW with Type I modification has been realized in a number of materials, e.g., borosilicate glass[25], aluminosilicate glass[26], and fused silica[27].

In our earlier works, we have fabricated 3D Type I waveguide beam splitters in $LiNbO_3$ crystal by FLW[28]. However, the beam

splitter was performed using a Y-junction. These junctions have inherent losses due to imperfection of crotch structures. Therefore, it is worth trying an alternative solution on a beam splitter with evanescent field coupling. As of yet, there have been very few reports on the manufacture and characterization of Type I waveguide couplers in $LiNbO_3$ crystals by FLW.

In this work, to compare guided wave performance between a directional waveguide coupler beam splitter and a Y-junction waveguide beam splitter, we present on the fabrication of Type I waveguide couplers by FLW in z-cut $LiNbO_3$ crystal, including two-dimensional (2D, one to two) and 3D (one to four) configurations. The guiding properties of the waveguide couplers are also experimentally and numerically studied at the wavelength of 632.8 nm, such as those previously reported in Ref. [27].

2. Experimental Details

The z-cut $LiNbO_3$ crystal was cut with a size of 10 mm (x) × 10 mm (y) × 1 mm (z) and with all of the faces polished to optical quality. The waveguide couplers were micromachined by FLW, as shown on the left of Fig. 1. An optical fiber laser system (origami-10XP, OneFive) generating a pulse laser beam with 420 fs pulse duration, 1031 nm central wavelength, and 50 kHz repetition rate was utilized as the laser source. The pulse energy was controlled by a computer connected with the laser facility. The femtosecond laser pulses were focused through a 40× microscope objective (NA = 0.6) into the substrate beneath one of the 10 mm × 10 mm surfaces at the approximately 150 μm point. During the irradiation process, the prepared $LiNbO_3$ crystal was mounted at the xyz motorized stage controlled by a computer and was moved at a uniform and relatively high velocity of 4 mm/s along the y axis, which produced a damage track inside the sample. The pulse energy radiated on the $LiNbO_3$ crystal was set to 5.3 μJ. In this work, a single-line waveguide (to measure the change of the refractive index for all the waveguide couplers), three 2D (one to two) waveguide couplers, and a 3D (one to four) waveguide coupler were manufactured, respectively. Metalloscopy (Axio Imager, Carl Zeiss) was utilized to image the cross sections of all the waveguide couplers. For the 2D waveguide couplers, the input waveguide of 7 mm long was isolated from two output waveguides of 7 mm long with center-to-center separation distances, Sc, of 4 μm (C1), 8 μm (C2), and 12 μm (C3), respectively. As the total length of the material is 10 mm, the coupling length of all the 2D waveguide couplers was 4 mm. For the 3D waveguide coupler, the input waveguide of 7 mm long was isolated from four output waveguides of 7 mm long with center-to-center separation distance of 8 μm.

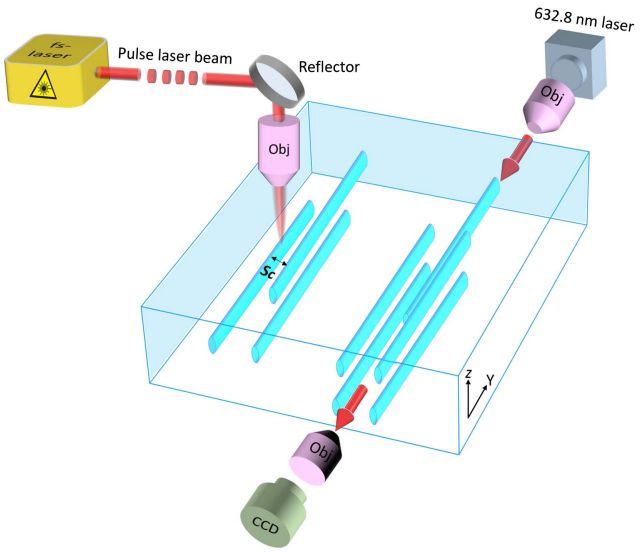

Fig. 1. Schematic process of FLW of the $LiNbO_3$ waveguide couplers (left). Schematic end-face coupling arrangement for investigation of the waveguide couplers at 632.8 nm (right).

The near-field modal profiles of the waveguide couplers were implemented with an end-face coupling experiment, also as shown on the right of Fig. 1. A He–Ne laser generating a wavelength of 632.8 nm laser beam was used for the probe source, and a half-wave plate was utilized to control the polarization of the incident laser beams. A pair of objective lenses (NA = 0.4) were employed to couple the light beam with a Gaussian spatial distribution into and out of the waveguide couplers. Finally, a CCD camera was used to apperceive and record near-field modal profiles, and a power meter was to measure the light powers coupled in and out of the waveguide coupler end-facets at 632.8 nm. Hence, the propagation loss of the waveguide couplers could be worked out by considering the coupling loss between input light and coupler end-facets.

3. Results and Discussion

Figures 2(a)–2(d) depict the microscopic photographs of the output cross section of the single-line waveguide and 2D waveguide couplers C1, C2, and C3. The recorded near-field intensity distributions of the single-line waveguide and 2D waveguide couplers C1, C2, and C3 at a single wavelength of 632.8 nm are shown in Figs. 2(e)–2(h). As one can see, the cores of near-field intensity distributions of Type I waveguide and waveguide couplers cores were located into laser-induced tracks. Additionally, the obtained modal profiles supported fundamental modes. However, the near-field modal profiles of the single-line waveguide and 2D waveguide couplers C1, C2, and C3 were

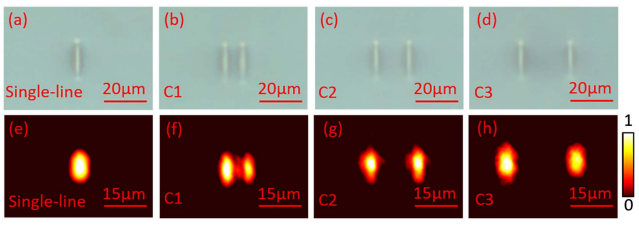

Fig. 2. Optical microscope images of the cross sections of (a) the single-line waveguide and waveguide couplers (b) C1, (c) C2, and (d) C3. The measured near-field intensity distributions at 632.8 nm of (e) the single-line waveguide and waveguide couplers (f) C1, (g) C2, and (h) C3 along TM polarization.

Table 1. Losses of the Single-Line Waveguide and Waveguide Couplers at 632.8 nm.

Waveguide	α (dB)	α_0 (dB)	α_1 (dB)	α_2 (dB)
Single-line waveguide	1.10	0.30	0.8	/
C1	1.62	0.63	0.8	0.19
C2	2.56	0.63	0.8	1.13
C3	4.53	0.63	0.8	3.10

only guided along the TM (n_e) polarization, and we cannot achieve the modal profile along TE (n_o) polarization, which agrees with the theoretical estimation of laser-written $LiNbO_3$ crystal[23].

The insertion losses α of the single-line waveguide (including propagation losses α_0 and coupling losses between the input light and the guided mode α_1) and the waveguide couplers C1, C2, and C3 (including α_0, α, and coupling loss between the input waveguide and the output waveguide α_2) at wavelength of 632.8 nm are depicted in Table 1. Considering the overlap of model profiles between the incident light beam and waveguide modes, the α_1 of all waveguides was estimated to be 0.8 dB due to same size of the input waveguides with the calculation method in Ref. [29]. Therefore, the propagation loss of the single-line waveguide is 0.3 dB/cm. Due to the same fabrication parameter of all waveguides, the values of the propagation losses α_0 ultimately depends on the waveguide length; thus, the propagation losses of the single-line waveguide (the waveguide length 10 mm) and waveguide couplers (the waveguide length 7 × 3 mm) were 0.3 dB and 0.63 dB. Apparently, as the separation of two coupled transmission lines increases, the coupling losses α_2 between the input waveguide and the output waveguide of the waveguide couplers become larger, which may be induced by the weak coupling between the input port and output port. The coupling losses of waveguide couplers can be further reduced by reducing these separation distances and changing the coupling length. As of yet, the 2D waveguide couplers C1 and C2 exhibit excellent performances of lower losses for beam splitters[28].

Assuming a step-like refractive index profile, the contrast of refractive index (Δn) of the single-line waveguide was estimated by measuring the NA. Through measuring the maximum incident angle Θ_m of the single-line waveguide where there is no change in transmission power, the maximum Δn increase was calculated by employing the formula[30]

$$\Delta n \approx \frac{\sin^2 \theta_m}{2n}, \tag{1}$$

where n represents n_e or n_o, and $n_e = 2.202$ is the refractive index of the substrate at 632.8 nm[31]. In this work, due to all the waveguides with the same preparation parameters, the calculated maximum Δn was 9.5×10^{-4} for all waveguide couplers.

For 12 μm waveguide separation, high losses would impede the propagation of the 3D waveguide coupler in $LiNbO_3$ crystal.

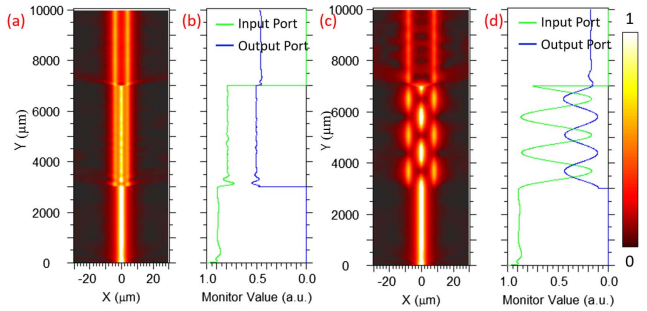

Fig. 3. *xy*-plane beam propagation simulation (RSoft) of 3D waveguide couplers (a) C1 and (c) C2 in $LiNbO_3$ crystal. Monitored 632.8 nm light guided in each coupler arm along the 3D waveguide couplers (b) C1 and (d) C2.

To determine whether to use 4 μm Sc or 8 μm Sc for the fabrication of 3D waveguide couplers, we simulated the light propagation of C1 and C2 by using BeamPROP (Rsoft, Inc.) software at 632.8 nm, which is based on the finite-difference beam propagation method (FD-BPM)[32] and the obtained Δn. Figures 3(a) and 3(c) show the simulated *xy*-plane beam propagation model of the 3D waveguide couplers with 4 μm Sc and 8 μm Sc, respectively. The amount of light in the input arm and output arms is monitored, as shown in Fig. 3. As Fig. 3(a) depicts, when the light passes into the output arms of the coupler, it is obvious that small separation distance could not separate the models from each other. Subsequently, the models of output waveguides have partial overlap between the output ports, which are in good concern with the experimental result of the 2D waveguide coupler C1 in Fig. 2(d). As the numerical simulation in Figs. 3(c) and 3(d) shows, the light is in an oscillation mode between two output waveguides for the 8 μm waveguide coupler C2, which may be caused by the limitations of numerical simulation, such as uncertainty in the refractive index line shape, or by the structure of the coupler, such as coupling length and coupling separation. Further reduction of the oscillation mode may be realized by optimization of numerical simulation methods and coupler construction. However, for the 8 μm waveguide separation, all light was isolated and restricted into the output arms or input arm with an oscillating mode when light propagated into the area of intercoupling, as depicted in Figs. 2(c) and 3(c). Although the output power of the 4 μm Sc coupler was higher than the 8 μm Sc coupler by comparing monitor value of the blue line in Fig. 3(b) and that in Fig. 3(d), the individual waveguide modes were imperative as a beam splitter. Therefore, we fabricated the 3D waveguide coupler with 8 μm separation along the *x* direction and *z* direction.

Figure 4(a) shows the microscopic photograph of the output cross section of the 3D waveguide coupler C4. The measured near-field model profile at 632.8 nm along the TM polarization is shown in Fig. 4(b). The propagation loss was measured to be 2.68 dB/cm at 632.8 nm. Figure 4(c) shows the simulated evolution process of modal profile following light beam propagation along the *z* axis of the waveguide coupler C4 at 632.8 nm. By comparing the shapes of modal profiles in Fig. 3(b) and the last simulated profile in Fig. 4, one can see that the measured profiles correspond with the experimental results, which proves that the

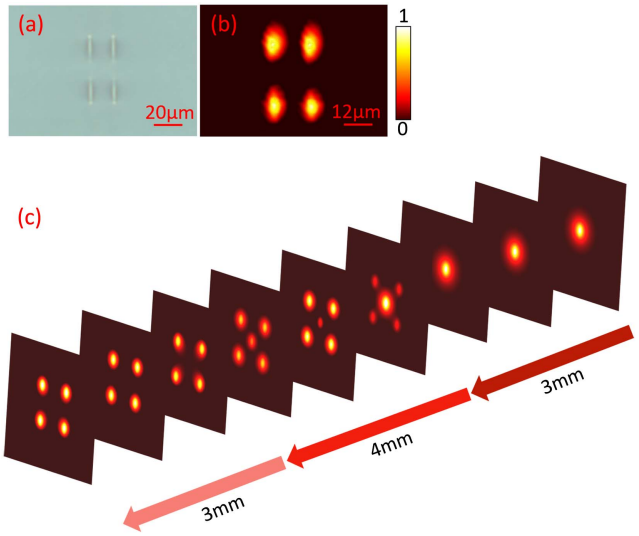

Fig. 4. (a) Microscopic photograph of the cross section, (b) measured near-field modal profile along TM polarization at 632.8 nm, and (c) simulated modal profile evolution of the 3D waveguide coupler C4.

calculated refractive index change of the waveguide coupler is reasonable. For the waveguide coupler C4, the measured splitting ratio for the four output ports is nearly equal with value of 49:50:47:46 at 632.8 nm, indicating that the manufactured 3D waveguide coupler has ability to be a 3D power splitter. Consequently, the splitting ratio and propagation loss could be further optimized by designing the laser-writing parameters and process. As our previous works mentioned, we have fabricated 2D and 3D Type I waveguide splitters with a Y-junction configuration in $LiNbO_3$ crystal, and output arms of the two waveguide splitters have the same lateral separation and the same preparation[28]. Additionally, the propagation losses reported for the 2D and 3D waveguide splitters were 3.45 dB/cm and 3.61 dB/cm, respectively, which were larger than that of waveguide coupler splitters. To have a more precise comparison of guided wave performance between the directional waveguide coupler beam splitter and the Y-junction waveguide beam splitter and to exclude the factors of processing parameters, we calculated the propagation losses change ($\Delta\alpha$) of different dimensions but with the same preparation condition, i.e., the $\Delta\alpha$ between the 2D and 3D waveguide splitters in same sample. As a result, the obtained additional loss of the Y-junction splitters was 0.16 dB/cm due to imperfection of the crotch in the Y-junction structures. The $\Delta\alpha$ of waveguide splitters with the type of evanescent field couplers was 0.12 dB/cm. Further reduction of $\Delta\alpha$ and splitting ratios closer to one may be realized by the design of FLW and processing parameters. The results indicate that our fabricated waveguide couplers, as a beam splitter, exhibit better transmission properties than Y-junction waveguide splitters.

4. Conclusion

In conclusion, we propose the design and fabrication of 2D and 3D waveguide couplers in $LiNbO_3$ crystal by FLW based on the Type I waveguide. The experimentally measured near-field modal profile and beam propagation model of the 3D waveguide coupler are in good agreement with the simulation results, and the splitting ratio of the 3D waveguide coupler is almost equalized. The results imply that our fabrication of 3D waveguide couplers can be applied to integrated photonic circuits. Additionally, the FLW technique shows promising capability for fabricating intricate photonic components or modules.

Acknowledgement

This work was supported by the National Natural Science Foundation of China (NSFC) (Nos. 20211062020035 and 12005147) and Postdoctoral Research Grants (No. 20211063010003).

References

1. F. Yu, T. C. Tzu, J. Gao, T. Fatema, K. Sun, P. Singaraju, S. M. Bowers, C. Reyes, and A. Beling, "High-power high-speed MUTC waveguide photodiodes integrated on Si_3N_4/Si platform using micro-transfer printing," IEEE J. Sel. Top. Quantum Electron. **29**, 3800106 (2022).
2. J. Čtyroký, J. Petráček, V. Kuzmiak, and I. Richter, "Bound modes in the continuum in integrated photonic $LiNbO_3$ waveguides: are they always beneficial?" Opt. Express **31**, 44 (2023).
3. A. U. Rehman, Y. Khan, M. Irfan, and M. A. Butt, "Investigation of optical-switching mechanism using guided mode resonances," Photonics **10**, 13 (2022).
4. W. Ho, H. Chan, and K. Yang, "Planar optical waveguide platform for gas sensing using liquid crystal," IEEE Sens. J. **13**, 2521 (2013).
5. C. Y. Liu, "Tunable ultrashort electro-optical power divider using coupled photonic crystal waveguides," J. Mod. Opt. **59**, 218 (2012).
6. T. X. Tran and X. N. Nguyen, "Sharp switching in optical couplers with variable coupling coefficient," J. Lightwave Technol. **32**, 1565 (2014).
7. J. S. Kim and J. T. Kim, "Silicon electro-optic modulator based on an ITO-integrated tunable directional coupler," J. Phys. D **49**, 075101 (2016).
8. C. Li, "Electrooptic switcher based on dual transverse Pockels effect and lithium niobate crystal," IEEE Photon. Technol. Lett. **29**, 2159–2162 (2017).
9. K. Buse, A. Adibi, and D. Psaltis, "Non-volatile holographic storage in doubly doped lithium niobate crystals," Nature **393**, 665 (1998).
10. P. Kharel, C. Reimer, K. Luke, L. He, and M. Zhang, "Breaking voltage–bandwidth limits in integrated lithium niobate modulators using micro-structured electrodes," Optica **8**, 357–363 (2021).
11. Y. Liu, X. Huang, Z. Li, H. Guan, Z. Yu, Q. Wei, Z. Fan, W. Han, and Z. Li, "On-chip four-mode (de-)multiplexer on thin film lithium niobate-silicon rich nitride hybrid platform," Opt. Lett. **46**, 3179 (2021).
12. Z. Chen, Q. Xu, K. Zhang, W. H. Wong, D. L. Zhang, E. Y. P. Pun, and C. Wang, "Efficient erbium-doped thin-film lithium niobate waveguide amplifiers," Opt. Lett. **46**, 1161 (2021).
13. R. C. Twu, "Zn-diffused $LiNbO_3$ 2× 2 balanced-bridge optical switch with post thermal-treatment," Microw. Opt. Technol. Lett. **41**, 493 (2004).
14. P. Hua, E. Y. Pun, D. Yu, and D. Zhang, "Nonperiodic oscillation with wavelength of mode guided in a special Ti-Diffused $LiNbO_3$ waveguide structure," IEEE Photonics J. **5**, 2202307 (2013).
15. K. Baba and T. Nakai, "Design and theoretical characteristics of directional coupler-type optical polarization splitters using dielectric periodic multilayers," Proc. SPIE **7933**, 793320 (2011).
16. J. L. Jackel, C. E. Rice, and J. J. Veselka, "Proton exchange in $LiNbO_3$," Ferroelectrics **50**, 165 (1983).
17. Y. C. Yao, W. J. Wang, and B. Y. Zhang, "Designing MMI structured beam-splitter in $LiNbO_3$ crystal based on a combination of ion implantation and femtosecond laser ablation," Opt. Express **26**, 19648 (2018).

18. H. Tang, C. Di Carlo, Z. Y. Shi, T.-S. He, Z. Feng, J. Gao, K. Sun, Z.-M. Li, Z.-Q. Jiao, T.-Y. Wang, M. S. Kim, and X.-M. Jin, "Experimental quantum fast hitting on hexagonal graphs," Nat. Photonics **12**, 754 (2018).
19. H. Xu, Y. Cheng, S. L. Chin, and H. B. Sun, "Femtosecond laser ionization and fragmentation of molecules for environmental sensing," Laser Photonics Rev. **9**, 275 (2015).
20. T. Huang, J. Lu, R. Xiao, Q. Wu, and W. Yang, "Enhanced photocatalytic properties of hierarchical three-dimensional TiO_2 grown on femtosecond laser structured titanium substrate," Appl. Surf. Sci. **403**, 584 (2017).
21. F. Flamini, N. Viggianiello, M. Bentivegna, N. Spagnolo, P. Mataloni, A. Crespi, R. Ramponi, R. Osellame, and F. Sciarrino, "Generalized quantum fast transformations via femtosecond laser writing technique," Interdiscip. Inf. Sci. **23**, 115 (2017).
22. S. Gross, M. Dubov, and M. J. Withford, "On the use of the Type I and II scheme for classifying ultrafast laser direct-write photonics," Opt. Express **23**, 7767 (2015).
23. F. Chen and J. R. Vazquez de Aldana, "Optical waveguides in crystalline dielectric materials produced by femtosecond-laser micromachining," Laser Photonics Rev. **8**, 251 (2014).
24. M. Heinrich, A. Szameit, F. Dreisow, S. Döring, J. Thomas, S. Nolte, A. Tünnermann, and A. Ancona, "Evanescent coupling in arrays of type II femtosecond laser-written waveguides in bulk *x*-cut lithium niobate," Appl. Phys. Lett. **93**, 101111 (2008).
25. M. Ams, R. J. Williams, and M. J. Withford, "Direct laser written waveguide coupler with an optically tunable splitting ratio," Proc. SPIE **7925**, 79250K (2011).
26. N. Riesen, S. Gross, J. D. Love, and M. J. Withford, "Femtosecond direct-written integrated mode couplers," Opt. Express **22**, 29855 (2014).
27. L. A. Fernandes, J. R. Grenier, P. Herman, J. Aitchison, and P. Marques, "Femtosecond laser fabrication of birefringent directional couplers as polarization beam splitters in fused silica," Opt. Express **19**, 11992 (2011).
28. J. Lv, Y. Cheng, W. Yuan, X. Hao, and F. Chen, "Three-dimensional femtosecond laser fabrication of waveguide beam splitters in $LiNbO_3$ crystal," Opt. Mater. Express **5**, 1274 (2015).
29. C. Cheng, C. Romero, J. R. Vazquez de Aldana, and F. Chen, "Superficial waveguide splitters fabricated by femtosecond laser writing of $LiTaO_3$ crystal," Opt. Eng. **54**, 067113 (2015).
30. J. Siebenmorgen, K. Petermann, G. Huber, K. Rademaker, S. Nolte, and A. Tünnermann, "Femtosecond laser written stress-induced Nd:$Y_3Al_5O_{12}$ (Nd:YAG) channel waveguide laser," Appl. Phys. B **97**, 251 (2009).
31. W. Atuchin and T. Khasanov, "High-accuracy contactless method for determination of chemical composition of lithium niobate crystals by their birefringence," Opt. Spectroscopy **107**, 212 (2009).
32. http://www.rsoftdesign.com.